

SIMULATIONS OF NANOINDENTATION IN A NON-CRYSTALLINE METAL FILM

Yunfeng Shi and Michael L. Falk

Department of Materials Science and Engineering, University of Michigan, Ann Arbor, MI 48109-2136 USA

ABSTRACT

A series of molecular dynamics simulations of nanoindentation in a two-dimensional model of a thin metallic glass film exhibit varying degrees of shear localization below the indenter depending on the means of glass processing. The indenter is circular, and all tests were performed at 9.2% of the glass transition temperature (T_g). The glasses were created from a melt 7.7% above T_g by: (I) quenching gradually over a period of approximately 0.5 μ s, (II) quenching quickly over a period of approximately 10 ns, and (III) quenching instantaneously from a well-equilibrated liquid state. Indentation was performed at approximately 0.3 m/s to a depth of 8nm. During nanoindentation shear bands nucleated at an indentation depth of approximately 15 \AA in the gradually quenched samples. In the shear band region material that previously exhibited local quasi-crystal-like structural ordering transformed into purely amorphous material under deformation. This structural transition appears to be related to the softening mechanism that results in strain localization in the material. Substantially less localization occurred in samples produced by higher rates of quenching.

1 INTRODUCTION

Metallic glasses can be produced by a variety of processing routes ranging from casting at relatively low cooling rates of a few Kelvin per second in the case of bulk glass formers [1, 2] to sputter quenching at elevated cooling rates [3] to ion beam processing, an extremely energetic non-equilibrium technique. Since glasses, unlike crystals, do not naturally conform to a small number of identifiable and well-defined ground state structures, it is generally expected that glasses can exhibit a range of mechanical properties depending on processing.

In addition it has long been established that localization plays an important role in the mechanical response of metallic glasses [4]. Recently a number of micro- and nano- hardness studies have demonstrated that shear localization results in characteristic surface features beneath the indenter [5-12]. These features are accompanied by a serrated response indicative of the bursts of deformation that accompany the nucleation of shear bands during loading. The mechanics of localization is understood to arise as a consequence of softening in the mechanical response during shear loading. This is often attributed to structural changes that also make deformation in amorphous solids apparently dilatant, requiring the use of pressure dependent constitutive laws such as the Mohr-Coulomb yield criterion. Interestingly localization and serrated behavior is not reported in studies of amorphous films generated by highly energetic processes [13].

Despite recent progress, however, understanding of the physical origin of the dilatancy and the softening mechanism remains rudimentary. While the most widely accepted theories [14-16] do provide important physical insight regarding the role of “free volume” and micromechanics in softening, none of these can be used to accurately model the nucleation and propagation of shear bands, and none of the parameters in the current theories can unambiguously be attributed to specific atomic scale structures or mechanisms. In many cases computer simulation studies have provided critical insight for theoretical progress [17, 18] and it is in the context of this work that the current study has been undertaken.

We have performed a series of nanoindentation simulations on three model metallic glass thin films. Because of the difficulty of modeling metallic glasses in their full complexity even on these small scales we have chosen to make a number of simplifying assumptions that preclude our

simulations from providing quantitative predictions, but that allow us to simulate large enough systems to obtain important physical insights into the deformation below the indenter. These simplifications include simulating a binary alloy, using a pair-potential interaction to model the metallic bonding, restricting our simulation to two-dimensions, operating at rates significantly above those typically observed experimentally and using glass preparation procedures at faster quench rates than are typically experienced in the laboratory. Despite these simplifications the results of the simulations exhibit most of the salient features of the experimental observations of indentation in metallic glasses. They also reveal some interesting trends regarding shear localization and metallic glass processing, and they provide a means to correlate deformation with atomic scale structural changes in the glass.

2 METHODOLOGY

We have performed molecular dynamics simulation on a binary alloy that consists of two species, which we will refer to as S and L for small and large, interacting via a Lennard-Jones potential of the form

$$\phi(r) = 4\epsilon \left[\left(\frac{\sigma}{r} \right)^{12} - \left(\frac{\sigma}{r} \right)^6 \right], \quad (1)$$

where ϵ represents the minimum energy of the bond and σ provides a length scale, the distance at which the interaction energy is zero. The SS and LL bond energies are half that of the SL bond energy, $\epsilon_{SS} = \epsilon_{LL} = \frac{1}{2} \epsilon_{SL}$. The SS and LL length scales are related to the SL length scale by

$$\sigma_{SS} = 2\sigma_{SL} \sin\left(\frac{\pi}{10}\right), \quad \sigma_{LL} = 2\sigma_{SL} \sin\left(\frac{\pi}{5}\right). \quad (2)$$

In this binary system we will take the reference length scale to be the σ value of the SL bond and the reference energy scale to be the energy of the SL bond. All the particles will have the same mass, m_0 , which will be the reference mass scale. The reference time scale will therefore be $t_0 = \sigma_{SL} \sqrt{m_0 / \epsilon_{SL}}$. In order to make rough comparisons to experiments and to present times in physical units we will consider that for a typical material $t_0 \approx 1$ ps, and $\sigma_{SL} \approx 3 \text{ \AA}$.

This system was chosen because it exhibits both crystalline and quasi-crystalline ground states [19]. The existence of a quasi-crystalline ground state was of particular interest because it has been proposed that such an underlying quasi-crystalline state stabilizes Zr based glasses, some of the most stable bulk glass formers produced to date [20, 21]. This system, perhaps due to this underlying quasi-crystalline state, exhibits a strong tendency toward amorphization. Many other two-dimensional systems show a strong tendency to crystallize. In addition this system has been used extensively to study quasi-crystal and amorphous thermodynamic and mechanical properties. We chose our composition $N_L:N_S = (1+\sqrt{5}):4$ to be consistent with other studies of this system. T_g of this system is known to reside around $0.325 \epsilon_{SL}/k$, where k is the Boltzmann factor. For the sake of comparison temperatures will be measured in units of this T_g .

The model system was simulated using a standard leapfrog integration scheme applied to the Newtonian equations of motion [22]. During quenching the coupling to the external heat bath was modeled using a Nose-Hoover thermostat. During indentation the same technique was used to maintain a constant temperature in the sample.

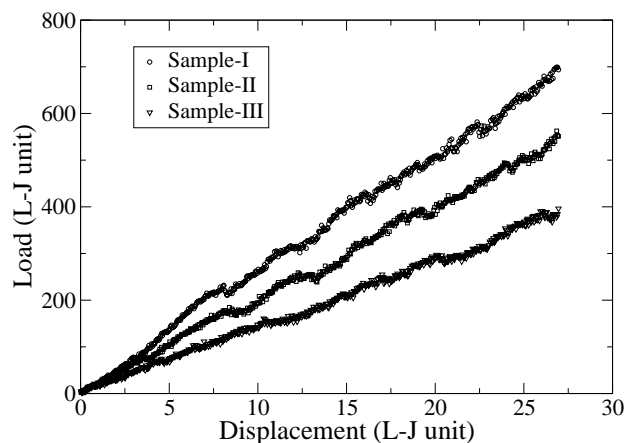


Figure 1: The load-displacement curves for three nano-indentation simulations performed on samples that were quenched gradually (I), quickly (II) and instantaneously (III).

3 SAMPLE PREPARATION AND TESTING

The initial conditions were created by starting from supercooled liquids equilibrated above the glass transition temperature. The relaxation time of the liquid was measured by tracking the decay of the structure factor. Liquids were equilibrated for many times this relaxation time. Subsequent to equilibration the temperature of the liquid was reduced to 9.2% of T_g . Sample I, the most gradually quenched sample, was cooled at a rate of $1.97 \times 10^{-6} T_g/t_0$, corresponding to a quench over approximately 0.5 μ s. Sample II, the intermediately quenched sample, was cooled at a rate of $0.98 \times 10^{-4} T_g/t_0$, corresponding to a quench over approximately 10 ns. Sample III, the least well-equilibrated sample, was quenched instantaneously by rescaling the particle velocities and then allowed to age for 100 t_0 , approximately 0.1 ns. These samples were then tiled 5 across by 2 down to create a single slab of 200,000 atoms which formed the $270 \sigma_{SL}$ or approximately 81 nm thick film. The indenter was composed by excising a section with a constant radius of curvature, $r=250 \sigma_{SL}$, approximately 75 nm.

During the indentation the indenter atoms were not allowed to move relative to each other. Therefore the indenter acts as a material of infinite stiffness. The slab was held between periodic boundaries on the right and left. The lower edge of the slab was held fixed as if the amorphous film were deposited upon a substrate of infinite stiffness. The indenter was lowered into the substrate under displacement control at a velocity of $0.001 \sigma_{SL}/t_0$ to a depth of $27 \sigma_{SL}$, approximately 0.3m/s to a depth of 8nm.

4 RESULTS

Fig. 1 shows the load displacement curves during loading for all three samples. The most robust feature of the load displacement curves is that the more gradually quenched the sample the higher the apparent hardness. In addition, the load displacement curve for sample III, the instantaneously quenched sample, is significantly smoother than the other two curves that each exhibit evidence of unsteady or serrated flow. This is surprising in light of recent studies which have claimed that at high loading rates serrated flow should be suppressed. The maximum loading

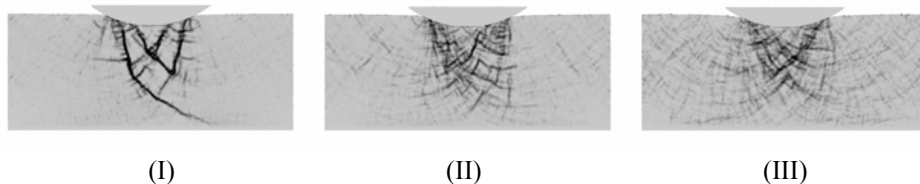


Figure 2: The three samples at the maximum indentation depth visualized by the amount of deviatoric strain. Gray corresponds to 0% strain; black corresponds to 40% strain.

rates for the experimental observation of serration are typically considerably lower than the loading rates simulated here. The implication is that the critical rate for serration is a function not simply of loading rate, but also of the composition and processing of the glass in question since in Fig. 1 we see evidence of both serrated and smooth flow for the same material composition but different processing methods. It is also important to note that the maximum indentation depth in these studies is approximately 8nm, significantly higher in resolution than a typical experimental nanoindentation study.

In order to directly examine the onset of plastic flow below the indenter we have extracted the local strain in the vicinity of each atom in the glass. This was done using the procedure for extracting a best fit strain introduced in [22]. Fig. 2 shows images of the regions of high deviatoric strain in each sample at the maximum indentation depth. Sample I shows evidence of localized deformation underneath the indenter. The first shear bands nucleate at a displacement of $8 \sigma_{SL}$, approximately 24 Å. This corresponded to an indentation depth of $4.9 \sigma_{SL}$, approximately 15 Å. Shear bands carry the majority of the plastic flow in this sample. Sample II exhibits the majority of deformation in a region immediately beneath the indenter, but the plastic flow is significantly less localized than in sample I. Sample III exhibits deformation both underneath the indenter and in regions quite far from the indenter. This is a consequence of the unstable nature of sample III; the energy per particle decreases with deformation in this sample because the glass was instantaneously quenched.

Fig. 2 shows how the samples have undergone deformation, but does not provide any information regarding the changes in structure that accompany deformation. To accomplish this we have adapted an analysis from [23] that utilizes the fact that this system has an underlying quasi-crystalline ground state. In [23] it was noticed that the quasi-crystal is composed of nine local atomic motifs. We have examined the structure of the samples, and we have determined if each atom resides in one of these motifs. Before indentation sample I has 74% of its atoms in stable motifs; sample II has 58% in stable motifs, and sample III has 44% in stable motifs. During indentation the number of atoms in stable motifs decreases in samples I and II and increases in sample III. The spatial distributions of stable and unstable atoms after indentation are shown in Fig. 3. It is apparent that in sample I the shear bands coincide with regions in which atoms are no longer in stable motifs. In sample II a more subtle increase in unstable atoms is evident under the indenter. In sample III no correlated spatial inhomogeneities are evident under the indenter.

5 CONCLUSIONS

We have performed a series of nanoindentation simulations on binary models of a glass forming system in two dimensions. More gradually quenched samples appear to have larger degrees of

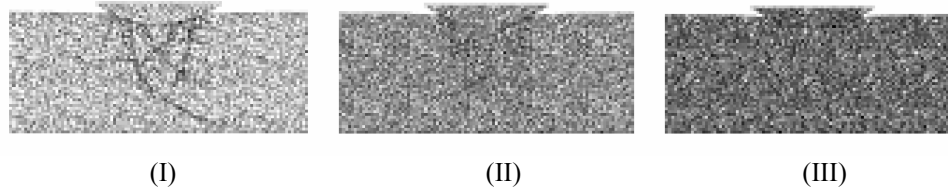


Figure 3: The three samples at the maximum indentation depth visualized by the percent of atoms with quasi-crystalline order. White corresponds to 100% quasi-crystalline order; Black corresponds to no quasicrystalline order.

quasicrystalline order. These samples also show an increasing tendency to exhibit shear band formation underneath the indenter. The formation of shear bands has been observed to coincide with the conversion of material away from the stable motifs that are typical of the quasi-crystalline arrangement. This study raises a series of important questions for understanding metallic glass structure and the mechanical response of apparently amorphous solids.

A number of the more stable metallic glass formers precipitate quasi-crystals upon annealing. It has been proposed that small regions with quasi-crystalline order may be important for the stability of the amorphous state in these glasses [20, 21]. In addition it has been asserted that deformation takes place primarily in the amorphous region of the material [24]. In our model system we have observed that the dispersed quasi-crystalline phase plays a critical role in controlling the qualitative nature of deformation in the material. In the material that shows the strongest tendency to form shear bands deformation converts material from quasi-crystal-like to fully amorphous. This implies that this conversion of material to the amorphous state may play a crucial role in the softening process that leads to the shear banding instability. However, it remains unclear whether this is true for all metallic glasses, or only those in which the stability of the amorphous phase arises from an underlying quasi-crystalline phase.

ACKNOWLEDGEMENTS

The authors would like to acknowledge the support of the U.S. National Science Foundation under grant DMR-0135009 and the donors of the American Chemical Society Petroleum Research Fund for support under grant 37558-G.

REFERENCES

1. Inoue, A., "Stabilization of metallic supercooled liquid and bulk amorphous alloys," *Acta Mater.* **48**, 279-306 (2000)
2. Johnson, W. L., "Bulk glass-forming metallic alloys: Science and technology," *MRS Bull.* **24**, 42-56 (1999)
3. Klement, W., Willens, R. H. and Duwez, P., "Non-Crystalline Structure in Solidified Gold-Silicon Alloys," *Nature* **187**, 869-70 (1960)
4. Pampillo, C. A. and Chen, H. S., "Comprehensive Plastic-Deformation of a Bulk Metallic Glass," *Mater. Sci. Eng.* **13**, 181-8 (1974)
5. Golovin, Y. I., Ivolgin, V. I., Tyurin, A. I. and Khonik, V. A., "Serrated deformation of a Pd40Cu30Ni10P20 bulk amorphous alloy during nanoindentation," *Physics of the Solid State* **45**, 1267-71 (2003)

6. Schuh, C. A., Argon, A. S., Nieh, T. G. and Wadsworth, J., "The transition from localized to homogeneous plasticity during nanoindentation of an amorphous metal," *Phil. Mag.* **83**, 2585-97 (2003)
7. Schuh, C. A. and Nieh, T. G., "A nanoindentation study of serrated flow in bulk metallic glasses," *Acta Mater.* **51**, 87-99 (2003)
8. Vaidyanathan, R., Dao, M., Ravichandran, G. and Suresh, S., "Study of mechanical deformation in bulk metallic glass through instrumented indentation," *Acta Mater.* **49**, 3781-9 (2001)
9. Wright, W. J., Saha, R. and Nix, W. D., "Deformation mechanisms of the Zr₄₀Ti₁₄Ni₁₀Cu₁₂Be₂₄ bulk metallic glass," *Mater. Trans.* **42**, 642-9 (2001)
10. Golovin, Y. I., Ivolgin, V. I., Khonik, V. A., Kitagawa, K. and Tyurin, A. I., "Serrated plastic flow during nanoindentation of a bulk metallic glass," *Scripta Mat.* **45**, 947-52 (2001)
11. Benameur, T., Hajlaoui, K., Yavari, A. R., Inoue, A. and Rezgui, B., "On the characterization of plastic flow in Zr-based metallic glass through micro-indentation: An atomic force microscopy analysis," *Mater. Trans.* **43**, 2617-21 (2002)
12. Jiang, W. H. and Atzmon, M., "Rate dependence of serrated flow in a metallic glass," *J. Mater. Res.* **18**, 755-7 (2003)
13. Zhao, B., Gao, Y., Zeng, F. and Pan, F., "Nanoindentation study of Ni₄₅Nb₅₅ amorphous films prepared by ion beam assisted deposition," *Nucl. Instrum. Methods B* **211**, 339-45 (2003)
14. Spaepen, F., "A Microscopic Mechanism for Steady State Inhomogeneous Flow in Metallic Glasses," *Acta metall* **25**, 407-15 (1977)
15. Steif, P. S., Spaepen, F. and Hutchinson, J. W., "Strain Localization in Amorphous Metals," *Acta metall.* **30**, 447-55 (1982)
16. Argon, A. S., "Plastic Deformation in Metallic Glasses," *Acta metall.* **27**, 47-58 (1979)
17. Srolovitz, D., Vitek, V. and Egami, T., "An Atomistic Study of Deformation of Amorphous Metals," *Acta metall.* **31**, 335-52 (1983)
18. Deng, D., Argon, A. S. and Yip, S., "Topological Features of Structural Relaxations in a 2-Dimensional Model Atomic Glass .2," *Philos. Trans. R. Soc. Lond. Ser. A-Math. Phys. Eng. Sci.* **329**, 575-93 (1989)
19. Lancon, F., Billard, L. and Chaudhari, P., "Thermodynamical Properties of a Two-Dimensional Quasi-Crystal from Molecular-Dynamics Calculations," *Europhysics Letters* **2**, 625-9 (1986)
20. Saida, J., Kasai, M., Matsubara, E. and Inoue, A., "Stability of glassy state in Zr-based glassy alloys correlated with nano icosahedral phase formation," *Annales De Chimie-Science Des Materiaux* **27**, 77-89 (2002)
21. Saksl, K., Franz, H., Jovari, P., Klementiev, K., Welter, E., Ehnes, A., Saida, J., Inoue, A. and Jiang, J. Z., "Evidence of icosahedral short-range order in Zr₇₀Cu₃₀ and Zr₇₀Cu₂₉Pd₁ metallic glasses," *Appl. Phys. Lett.* **83**, 3924-6 (2003)
22. Falk, M. L. and Langer, J. S., "Dynamics of viscoplastic deformation in amorphous solids," *Phys. Rev. E* **57**, 7192-205 (1998)
23. Widom, M., Strandburg, K. J. and Swendsen, R. H., "Quasi-Crystal Equilibrium State," *Phys. Rev. Lett.* **58**, 706-9 (1987)
24. Saida, J. and Inoue, A., "Microstructure of tensile fracture in nanicosahedral quasicrystal dispersed Zr₈₀Pt₂₀ amorphous alloy," *Scripta Mat.* **50**, 1297-301 (2004)